



Published in final edited form as:

Ophthalmic Surg Lasers Imaging. 2011 July ; 42(0): S85–S94. doi:10.3928/15428877-20110627-08.

The Use of Optical Coherence Tomography in Intraoperative Ophthalmic Imaging

Paul Hahn, MD, PhD, Justin Migacz, MS, Rachelle O'Connell, BS, Ramiro S. Maldonado, MD, Joseph A. Izatt, PhD, and Cynthia A. Toth, MD

Departments of Ophthalmology (PH, RO, RSM, CAT) and Biomedical Engineering (JM, JAI), Duke University, Durham, North Carolina

Abstract

Optical coherence tomography (OCT) has transformed diagnostic ophthalmic imaging but until recently has been limited to the clinic setting. The development of spectral-domain OCT (SD-OCT), with its improved speed and resolution, along with the development of a handheld OCT scanner, enabled portable imaging of patients unable to sit in a conventional tabletop scanner. This handheld SD-OCT unit has proven useful in examinations under anesthesia and, more recently, in intraoperative imaging of preoperative and postoperative manipulations. Recently, several groups have pioneered the development of novel OCT modalities, such as microscope-mounted OCT systems. Although still immature, the development of these systems is directed toward real-time imaging of surgical maneuvers in the intraoperative setting. This article reviews intraoperative imaging of the posterior and anterior segment using the handheld SD-OCT and recent advances toward real-time microscope-mounted intrasurgical imaging.

INTRODUCTION

Optical coherence tomography (OCT) is a rapid, noncontact, and noninvasive method of cross-sectional imaging. Since the development of OCT imaging almost 20 years ago,¹ there have been continually expanding clinical applications of this modality in diagnostic imaging of the retina and the anterior segment. Until recently, the use of OCT has been limited to the clinic setting. The ability of OCT to view anatomic relationships in three dimensions and in high resolution has made intraoperative use of OCT a natural application for this imaging system. The development of a handheld OCT scanner has enabled intraoperative OCT imaging in supine patients. Current efforts are also underway to develop microscope-mounted OCT scanners for real-time imaging during surgical maneuvers. This review will focus on the intraoperative and recent real-time intrasurgical use of OCT in ophthalmic imaging.

BACKGROUND

The first commercially available OCT machine was the Stratus OCT released in 1995 by Carl Zeiss Meditec (Dublin, CA). This OCT machine used a time-domain OCT (TD-OCT) detection system, which provided an axial resolution of 10 μm and an imaging rate of approximately 400 A-scans per second. TD-OCT systems enabled, for the first time, in vivo cross-sectional visualization of individual retinal layers without histologic sectioning.

The advent of SD-OCT eliminated the need for the axial movement of the scanning mirror required in TD-OCT, yielding improved resolution and speed. Current SD-OCT machines

Address correspondence to Cynthia A. Toth, MD, DUMC 3802, Durham, NC 27707. cynthia.toth@duke.edu.

provide an axial resolution lower than 5 μm and scan at up to and beyond 20,000 A-scans per second. With SD-OCT, retinal structures can be visualized with greater detail and three-dimensional renderings can be routinely produced.²

OCT imaging has been adopted as an important clinical tool in the diagnosis and management of ophthalmic diseases. OCT was initially optimized for the imaging of macular diseases using an 830-nm wavelength light source. There has been an explosion in published reports of OCT findings in a wide range of macular disease entities. OCT imaging of the retinal nerve fiber layer has also demonstrated clinical utility in the early detection of glaucomatous progression.³ The use of OCT in managing retinal disease and glaucoma has now become routine and is approaching standard of care.

OCT is also obtaining widespread use in the assessment of anterior segment disease. Anterior segment imaging with OCT was first reported in 1994⁴ using an 830-nm wavelength light source. Use of a longer wavelength laser of 1,310 nm was found to result in improved penetration through highly scattering structures, including the sclera and limbus,⁵ and has been adopted in commercially available anterior segment OCT systems. Slit-lamp adapted OCT systems have also been developed to facilitate OCT imaging of the anterior segment and, more recently, posterior segment in clinical practice.⁶

OCT IMAGING IN PERIOPERATIVE MANAGEMENT

In addition to its role in diagnosis and management of clinical disease, OCT imaging has found an important role in preoperative surgical planning and our understanding of postoperative healing processes. OCT imaging has enabled visualization of anatomic pathology difficult to detect clinically. Gallemore et al. demonstrated greater sensitivity of OCT compared to biomicroscopy in the detection of vitreomacular adhesions,⁷ which may benefit from surgical intervention. In another study, OCT was useful in defining the three-dimensional configuration of vitreomacular adhesions, which was important in planning the surgical approach to access the subhyaloid space.⁸ OCT has become the gold standard in the preoperative identification of full-thickness macular holes and is particularly useful in differentiating full-thickness holes from inner lamellar or pseudoholes.⁹ Postoperative recovery following macular hole surgery, including the course of macular hole closure and postoperative positioning requirements, has additionally been closely examined using OCT imaging.¹⁰

Anterior segment OCT has also proven extremely useful in the clinical evaluation and perioperative management of anterior segment procedures. Visualization of the depth of corneal scars with anterior segment OCT has been important in guiding selection of surgical management with either lamellar or penetrating keratoplasty.¹¹ In patients undergoing lamellar keratoplasty, anterior segment OCT can image the position of the donor graft following transplantation with visualization of the donor–host interface.¹² Anterior segment OCT has also developed a critical role in refractive surgery. Anterior segment OCT can accurately measure the thickness of LASIK flaps and residual stroma,¹³ which may be important in predicting postoperative outcomes and in evaluating eligibility of patients for post-LASIK enhancement.¹⁴

IMAGING WITH THE HANDHELD OCT

The development of a portable, handheld SD-OCT scanner in 2007 (Bioptigen, Inc., Research Triangle Park, NC) enabled imaging of patients unable to sit upright in a conventional tabletop scanner. This SD-OCT system contains a handheld imaging handpiece that is adapted to a light source of 840-nm wavelength and can produce high-resolution images with an axial resolution less than 5 μm . The handheld OCT scanning head can

operate while positioned at any angle and thus is useful for scanning the supine patient. This handpiece is connected via a 1.3-m flexible fiberoptic cable to a moveable cart housing the SD-OCT system with computer and viewing screen. The reference arm and dioptic correction are manually adjusted to image a range of adult and pediatric eyes.

Pediatric Imaging

The initial clinical application of the handheld SD-OCT device was in imaging pediatric patients. Prior to the development of a handheld SD-OCT system, there had been several reports of successful imaging of pediatric patients with the Stratus tabletop TD-OCT system¹⁵⁻²³ and a report with the Cirrus tabletop SD-OCT system (Carl Zeiss Meditec, Jena, Germany).²⁴ In these reports, the youngest child imaged was 3 years old. Imaging of younger patients in the clinic was limited by positioning and attention requirements of patients undergoing OCT imaging in a conventional tabletop scanner. There are also reports of TD-OCT imaging of pediatric patients with retinopathy of prematurity during examinations under anesthesia.^{25,26} There are clear positioning difficulties in imaging an anesthetized supine patient in a conventional tabletop OCT system,²⁷ and the methods of imaging during examinations under anesthesia were not elaborated in these reports.

The development of the Biotigen handheld SD-OCT system, with its handheld scanner and increased imaging speed, was important in facilitating high-resolution ophthalmic imaging of pediatric patients. This handheld SD-OCT system has been reported to successfully image retinas of full-term infants with shaken baby syndrome,^{28,29} albinism,³⁰ and retinopathy of prematurity,³¹ detecting retinal abnormalities not observed clinically with biomicroscopy. These studies were performed in infants under sedation with general anesthesia in the operative suite. Retinal imaging in non-sedated pediatric patients was also demonstrated with the Biotigen handheld OCT system in infants affected with retinopathy of prematurity³² and in normal children of various ages.³³ Scanning parameters and recommended scanning protocols have been optimized for the Biotigen system in non-sedated premature neonates and young children in the neonatal intensive care unit.³⁴

Recently, adaptation of the Heidelberg (Heidelberg Engineering, Heidelberg, Germany) Spectralis SD-OCT system has been reported to enable reproducible imaging of complex pediatric retinal diseases during examinations under anesthesia.³⁵ Vinekar et al. have also described the modification of the tabletop Heidelberg Spectralis SD-OCT device to allow handheld OCT imaging of non-anesthetized infants with retinopathy of prematurity.³⁶ By disassembling the tabletop system, the authors were able to free the scanning device from its tabletop mount and convert it into a large handheld scanner, which they used to image non-anesthetized supine infants in the clinical setting.

Intraoperative Retinal Imaging

Intraoperative handheld OCT imaging in supine patients undergoing surgery was an inevitable extension of pediatric imaging during examinations under anesthesia. Currently, intraoperative OCT imaging with the Biotigen handheld scanner employs a mobile OCT scanning station that is positioned in close proximity to the supine patient (Fig. 1). The handheld scanner, wrapped in a sterile covering, is connected by a fiberoptic cable to the station. While an assistant operates the computer software, the surgeon stabilizes the handpiece over the eye of interest to obtain images. The handpiece can be stabilized with either several fingertips against the patient's forehead or a fixed armature. A custom mount has also been described that stabilizes the handpiece against the surgical microscope and allows pivoting of the handpiece into imaging position for greater stabilization and imaging efficiency (Fig. 2).^{37,38}

In 2009, Dayani et al. reported the use of the Biotigen handheld SD-OCT to compare intraoperative pre-incision retinal images of patients undergoing surgery for macular disease, including full-thickness macular hole, epiretinal membrane (ERM), and vitreomacular traction, to images immediately following internal limiting membrane (ILM) or ERM peel (Fig. 3).³⁹ Following removal of the ILM or ERM with the Tano diamond-dusted membrane scraper and/or forceps, instruments were removed from the eye and the vitrectomy ports plugged. The handheld Biotigen scanner was then placed over the operative eye by the surgeon to obtain noncontact OCT imaging followed by completion of the surgical procedure.

Dayani et al. reported the technical difficulties and steep learning curve in obtaining high-resolution intraoperative images. Adequate stabilization of the handheld scanner was performed with fingertips against the subject's forehead and was critical in reducing motion artifact. Sufficient lubrication of the cornea was important in maintaining image resolution. Orientation of images was difficult but improved through larger scanning areas and visualization of axial summed voxel projections.

Despite these difficulties, Dayani et al. demonstrated that intraoperative SD-OCT imaging could be safely and efficiently performed. Their intraoperative images highlighted the presence of surgery-induced traumatic changes to the retinal surface. Residual ILM or ERM that was not easily visualized under the surgical microscope could be visualized intraoperatively, guiding further complete peeling of membranes. Intraoperative changes, including a mean size of the macular hole immediately following ILM peel and normalization of retinal contour following ERM peel, was also demonstrated for the first time by intraoperative OCT.

In a subsequent case report, Wykoff et al. described intraoperative Biotigen handheld SD-OCT findings in a child undergoing traumatic full-thickness macular hole surgery, demonstrating near complete closure of the hole following ILM peeling.⁴⁰ Lee and Srivastava reported two cases of intraoperative Biotigen hand-held imaging performed during rhegmatogenous retinal detachment repair.⁴¹ Images obtained intraoperatively following placement of perfluorocarbon liquid demonstrated residual subretinal fluid despite the appearance of an attached retina that persisted postoperatively under silicone oil.

Recently, Ray et al. reported a retrospective analysis of intraoperative Biotigen handheld SD-OCT imaging performed with their custom microscope mount (Fig. 2).³⁸ Thirteen consecutive eyes of 13 patients undergoing macular hole repair were imaged intraoperatively immediately following surgical maneuvers along with 12 consecutive eyes of 11 patients undergoing ERM peeling. Of these 25 eyes, images were considered insufficient for analysis in two patients undergoing macular hole repair. In the remainder of eyes, qualitative and quantitative analysis of images was performed, revealing an increase in subretinal fluid following ILM peeling and the development of a new subfoveal hyporeflectivity consistent with a shallow macular detachment following ERM peeling. In addition to providing novel information about anatomic changes during vitreoretinal surgery, this report confirms the feasibility of efficient intraoperative SD-OCT imaging and demonstrates the applicability of these images for quantitative analysis.

Intraoperative Anterior Segment Imaging

Although much of the development of intraoperative OCT has focused on retinal imaging, investigations have recently been directed toward intraoperative OCT imaging of the anterior segment. Knecht et al. used the Biotigen handheld SD-OCT to image the host-graft interface of corneas undergoing Descemet's stripping automated endothelial keratoplasty (DSAEK) surgery.⁴² The authors demonstrated that the handheld SD-OCT unit

is able to safely image the anterior segment and noted a steep learning curve to efficient imaging. They imaged the interface space between the endothelial graft and the host cornea, demonstrating that the graft can successfully adhere to the host cornea despite the presence of fluid in the interface at the end of surgery.

Ide et al. developed a prototype anterior segment SD-OCT device with a 1,310-nm wavelength superluminescent diode laser source and a spectrometer developed by Biotigen, Inc.⁴³ The scanner was mounted on a stabilizing arm connected to a mobile cart housing the computer workstation. This prototype achieved an axial resolution of 8 μm and was used to image the interface between the donor graft and the host cornea of patients undergoing DSAEK surgery. Residual interface fluid that was not detectable under the surgical microscope was identified in some patients, which was successfully aspirated followed by documented absence of residual fluid. The authors note that optimization of image quality and scan speed is required to improve their prototype system.

REAL-TIME INTRASURGICAL SD-OCT IMAGING

Although imaging of ocular structures intraoperatively was a natural application of the development of the handheld scanner, this technology was limited by the need to halt surgery to obtain images. In addition to the additional time required for surgery, this limitation prevents real-time imaging of ocular structures during surgical manipulations. The ability to visualize vitreoretinal or anterior segment structures in real time may improve the ease and success of current surgical interventions and may provide novel, important information regarding postoperative healing processes.

Microscope-Mounted OCT

Recently, there have been several independent groups working to develop SD-OCT systems capable of real-time intraoperative imaging during surgical manipulations.

At the time of writing this review article, the only published demonstration of successful imaging of vitreoretinal surgical maneuvers in model eyes has been reported by Tao et al.⁴⁴ The authors constructed a custom microscope-mounted OCT (MM-OCT) scanner. This MM-OCT unit was engineered to fit a Leica surgical microscope and to interface optically and mechanically with an Oculus Binocular Indirect Ophthalmic Microscope (BIOM), allowing the MM-OCT scanner to share the optical path of the surgical microscope to simultaneously image and visualize vitreoretinal surgical procedures.

This custom MM-OCT system used a superluminescent diode with a center wavelength of 840 nm to obtain images with an axial resolution in air of 6.51 μm . Critical to the design of the microscope was preservation of the surgeon's view through the operating microscope. The optical design magnified the SD-OCT beam to counteract the demagnification of the BIOM system and to preserve lateral resolution. The scan pivot was optically relayed to the iris plane of the patient to maximize field of view.

A dichroic mirror was placed in the infinity space of the optical path of the surgical microscope between the objective lens (orange box, Fig. 4) and beamsplitter and imaging optics of the microscope viewports (green path, Fig. 4). This mirror enabled folding of the SD-OCT beam (purple box, Fig. 4) into the microscope's optical path, allowing for a common focal plane between the OCT scanner and the surgical microscope. Software from Biotigen, Inc. was used to perform real-time data acquisition, processing, archiving, and display.

This MM-OCT design eliminates some of the limitations of intraoperative imaging using a handheld OCT system. By providing a stabilizing imaging arm with an optical path shared with the microscope, MM-OCT can image stably, quickly, and efficiently in the intraoperative setting. More important, the common optical path allows for real-time imaging of surgical maneuvers, unlike the handheld OCT system, which requires halting of surgery to obtain images. However, the MM-OCT is relayed through an extended optical system, including the microscope objective, reduction lens, and wide-field non-contact lens, resulting in potential signal reduction and aberrations due to suboptimal performance of these optics at the OCT wavelength of 840 nm.

Using this MM-OCT system, Tao et al. imaged the human fundus of healthy volunteer control subjects lying in a supine position to simulate conditions during vitreoretinal surgery. The authors applied 700- μ W illumination power at the pupil with imaging sessions lasting less than 5 minutes. This exposure lies well within the ANSI limits of less than 700 μ W of continuous-wave power in the 800 to 900 nm spectral range, which is allowable for continuous exposure for up to 8 hours.⁴⁵⁻⁴⁷ They also imaged vitreoretinal surgical manipulations in fresh cadaveric porcine eyes. The surgeon viewed the maneuvers through the surgical microscope with the MM-OCT in place, and the OCT images were displayed on a separate computer screen. Vitreoretinal surgical instruments could be imaged while interfaced with the postmortem retina (Fig. 5), documenting the variable reflectivity of instruments and the impact of shadowing on views of the underlying retina. Using the same MM-OCT system, Ehlers et al. compared reflectivity and shadowing characteristics of vitreoretinal microsurgical instruments composed of different materials.⁴⁸ Metallic instruments exhibited high reflectivity and total shadowing, whereas polyamide and silicone materials permitted greater visualization of underlying structures (Fig. 6).

This MM-OCT system is currently an early prototype system and needs further refinements before seamless intraoperative imaging of surgical maneuvers can be performed in human subjects. The current MM-OCT prototype displays OCT images on a display monitor on a separate workstation, and integrated display options for the surgeon will be important. Specific OCT scanning protocols, instrumentation design, and hardware improvements will also likely improve future MM-OCT prototypes. Nonetheless, this platform has demonstrated that high-resolution, non-contact, real-time imaging of vitreoretinal surgical maneuvers is feasible.

Other OCT Approaches

In addition to the MM-OCT system, there are reports of other OCT systems designed for real-time intraoperative imaging during vitreoretinal procedures. Binder et al. have adapted a Carl Zeiss Meditec Cirrus SD-OCT, which uses an 830-nm light source, to the optical pathway of a Zeiss OPMI VISU 200 surgical microscope. They imaged various steps of vitreoretinal and cataract surgery and were able to describe foveal morphology following ERM and ILM peel and following cataract extraction. They also imaged retinas during retinal detachment repair, noting subclinical fluid accumulation in the macula under silicone oil. These results were presented at the Association for Research in Vision and Ophthalmology meeting in 2010⁴⁹; at the time of writing of this review article, published reports and further details of their system were not available.

Instead of coupling an OCT scanner to the optical path of the surgical microscope, another group has approached intraoperative OCT imaging by developing an OCT scanner on a small-gauge probe with a 1,310-nm wavelength light source. Han et al. reported the use of a 21-gauge handheld forward-imaging OCT needle endoscope that was able to successfully image the vitreous, retina, and choroid of cadaveric pig eyes with an axial resolution of 10.5 μ m.⁵⁰ Although the authors propose intraoperative application of this system, reports of

real-time intraoperative imaging with this OCT endoscope have not been published. Similarly, Balicki et al.⁵¹ have reported the development of a 25-gauge microsurgical pick incorporating a single 125- μm diameter optical fiber interfaced to a custom SD-OCT unit. The authors have demonstrated the positioning ability of this pick to measure its distance from a model surface but have not yet demonstrated intraoperative application of this pick.

Imaging of the Anterior Segment

In 2001, Radhakrishnan et al. described the use of a 1,310-nm wavelength source coupled to a prototype handheld OCT scanner to perform real-time, high-speed, non-contact imaging in healthy volunteers of the anterior segment, including the cornea, angle, and iris.⁵² The potential intraoperative applications of this device were postulated by the authors, who predicted a role for intraoperative OCT in anterior segment imaging.

In 2005, Geerling et al.⁵³ reported the coupling of a commercially available 1,310-nm TD-OCT system (4Optics, Lübeck, Germany) with a dielectrical mirror to a surgical microscope (Hi-R 900; Möller-Wedel, Wedel, Germany). The authors were able to capture two-dimensional images of the anterior segment angle during trabeculectomy and of the cornea during deep anterior lamellar keratoplasty. These images were obtained intraoperatively and during surgical manipulation in human patients. Surgical instruments caused significant reflection and shadowing. The authors noted additional substantial limitations of their system, including the inability to orient the direction of the scanning laser perpendicular to the surface of interest and the poor penetration of their light source. Despite these limitations, their system demonstrated that a microscope-coupled OCT system could successfully image anterior segment structures intraoperatively during surgical manipulations.

Recently, Hüttmann et al. adapted an SD-OCT unit to the camera port of a surgical microscope.⁵⁴ The authors were able to image anterior segment structures in real time with visualization of instruments and incisions. They have stated that technical difficulties of intraoperative imaging have been solved and report the initiation of a clinical trial in the near future. Kermani et al. reported on the use of a custom OCT (Thorlabs HL AG, Lübeck, Germany) operating at a 930-nm wavelength to control depth of LASIK flaps cut with the femtosecond laser in cadaveric human eyes.⁵⁵ The OCT system was able to monitor creation of the LASIK flap in real time, permitting the visualization of flap as it was cut just below Bowman's layer.

FUTURE DIRECTIONS

The intraoperative use of OCT imaging is currently an area of intense development and will certainly be an important tool for posterior and anterior segment surgeries in the near future. Limitations of current systems will need to be addressed before these systems will allow seamless imaging.

Visualization of retinal manipulation has been limited by the reflectivity and backshadowing of current instrumentation. Ehlers et al. reported improved but still limited visualization of underlying structures with polyamide and silicone tips compared with metallic tips.⁴⁸ Characterization of the reflectivity and shadowing characteristics of different instruments and various materials will need to be refined to optimize OCT visibility of underlying structures. Development of forceps and other instruments with polyamide or silicone tips may be useful, and identification of novel instrument materials may further improve visibility.

Image quality can be improved by increasing strength of the light source with minimization of signal loss through the extended optical systems, but light source intensity must be carefully limited to minimize risk of possible light-induced toxicities. Currently, the most conservative ANSI requirements limit maximum exposure to less than 700 μW of continuous-wave power in the 800- to 900-nm spectral range through a 7-mm pupil aperture for continuous exposure of up to 8 hours.⁴⁵⁻⁴⁷ Real-time application of intrasurgical OCT systems must also consider additional light from the microscope or from fiberoptic endoillumination during vitreoretinal surgery. The impact of concurrent use of indocyanine green dye or other potentially phototoxic adjuvants will also need to be considered. OCT systems will need to maximize efficiency of their optical pathways while maintaining light exposure within safe limits. Contrast agents optimized for OCT imaging are being developed and may further improve visibility of ocular structures.⁵⁶

Feedback systems for the surgeon must be optimized and integrated into the surgeon's control. Current intraoperative OCT prototypes typically require an assistant to operate the OCT driving software and to perform manual, often time-consuming adjustments of the reference arm length. As these units are inevitably refined for commercial use, adjustments of the OCT scanner should be able to be performed by the surgeon, possibly through the use of additional foot-pedals or switches easily accessible to the surgeon.

Additionally, visualization options of the OCT images must be optimized. The data output of current OCT systems is voluminous and cannot be realistically processed instantaneously during surgical maneuvers. The development of tracking software to identify the location of instrument tips will likely prove useful in limiting OCT imaging to the area of interest. It will also be critical to identify information that is important for the surgeon in real time and to develop informatic display options for the surgeon. Currently, volume renderings and summed voxel projections can provide detailed spatial information, but real-time visualization is limited by the cumbersome and time-consuming software processing required to produce these images. Individual B-scans provide cross-sectional information but lack spatial information. The development of faster OCT technology, possibly using swept-source OCT, and of faster software processing algorithms may improve imaging and post-processing speed, which will be important in enabling real-time visualization of three-dimensional OCT renderings.

Display systems will also need to be developed that allow the surgeon to view OCT images in real-time during surgical maneuvers. Current systems typically involve a display monitor on a separate OCT workstation that is not visible to the surgeon without directing attention away from the surgical microscope. A heads-up display that integrates visualization of OCT images into the optical viewports of the surgical microscope may prove useful in safely and simultaneously displaying real-time cross-sectional OCT imaging with direct viewing of ocular structures.

A novel approach to intraoperative visualization of OCT images is the prototype OCT Penlight,⁵⁷ which uses a half-silvered mirror to project an in situ virtual image of a real-time OCT scan within the surgeon's line of sight. Testing of the OCT Penlight in ophthalmic surgical procedures has not been reported, but this innovative approach may prove useful, particularly for real-time visualization of anterior segment structures.

CONCLUSION

We are currently in the midst of a revolution in surgical imaging. The ability to provide high-resolution cross-sectional imaging of ocular structures has transformed clinical ophthalmic practice, and the use of OCT in the intraoperative setting has been a logical

progression from the use of this modality in the clinic. The development of spectral-domain OCT systems was important in improving resolution and speed of imaging. The production of a handheld SD-OCT unit enabled reproducible, high-resolution imaging of supine patients in the operative setting. Although the handheld OCT has yielded valuable information about surgical procedures and recovery processes, its inability to visualize ocular structures in real time during surgical maneuvers has limited its intraoperative applicability. OCT systems have recently been adapted to surgical microscopes, enabling real-time visualization of vitreoretinal and anterior segment surgical manipulations. Currently, these real-time OCT systems are in their early developmental stage. Significant improvements are aimed toward the seamless integration of real-time intraoperative imaging of ocular structures, which will undoubtedly revolutionize surgical practice within the next few years.

Acknowledgments

Supported by the Heed Ophthalmic Foundation (PH), NEI R21-EY-019411, and NCRR 1UL1 RR024128-01.

Dr. Izatt is a co-founder of Bioptigen, Inc. and has corporate, intellectual property, and equity interests in this company. Dr. Toth receives research support through equipment loan from Bioptigen and has potential for royalties for OCT-related technology licensed by Duke University to Bioptigen. Dr. Toth also receives royalties for surgical technology licensed by Duke University to Alcon Laboratories. Duke University has an equity interest in Bioptigen. The remaining authors have no financial or proprietary interest in the materials presented herein.

References

- Huang D, Swanson EA, Lin CP, et al. Optical coherence tomography. *Science*. 1991; 254:1178–1181. [PubMed: 1957169]
- Gabriele ML, Wollstein G, Ishikawa H, et al. Three dimensional optical coherence tomography imaging: advantages and advances. *Prog Retin Eye Res*. 2010; 29:556–579. [PubMed: 20542136]
- Schuman JS, Hee MR, Arya AV, et al. Optical coherence tomography: a new tool for glaucoma diagnosis. *Curr Opin Ophthalmol*. 1995; 6:89–95. [PubMed: 10150863]
- Izatt JA, Hee MR, Swanson EA, et al. Micrometer-scale resolution imaging of the anterior eye in vivo with optical coherence tomography. *Arch Ophthalmol*. 1994; 112:1584–1589. [PubMed: 7993214]
- Hoerauf H, Gordes RS, Scholz C, et al. First experimental and clinical results with transscleral optical coherence tomography. *Ophthalmic Surg Lasers*. 2000; 31:218–222. [PubMed: 10847499]
- Mueller M, Schulz-Wackerbarth C, Steven P, et al. Slit-lamp-adapted fourier-domain OCT for anterior and posterior segments: preliminary results and comparison to time-domain OCT. *Curr Eye Res*. 2010; 35:722–732. [PubMed: 20673049]
- Gallemore RP, Jumper JM, McCuen BW 2nd, Jaffe GJ, Postel EA, Toth CA. Diagnosis of vitreoretinal adhesions in macular disease with optical coherence tomography. *Retina*. 2000; 20:115–120. [PubMed: 10783942]
- Chung EJ, Lew YJ, Lee H, Koh HJ. OCT-guided hyaloid release for vitreomacular traction syndrome. *Korean J Ophthalmol*. 2008; 22:169–173. [PubMed: 18784444]
- Hee MR, Puliafito CA, Wong C, et al. Optical coherence tomography of macular holes. *Ophthalmology*. 1995; 102:748–756. [PubMed: 7777274]
- Jumper JM, Gallemore RP, McCuen BW 2nd, Toth CA. Features of macular hole closure in the early postoperative period using optical coherence tomography. *Retina*. 2000; 20:232–237. [PubMed: 10872926]
- Ma JJ, Tseng SS, Yarascavitch BA. Anterior segment optical coherence tomography for transepithelial phototherapeutic keratectomy in central corneal stromal scarring. *Cornea*. 2009; 28:927–929. [PubMed: 19654520]
- Ramos JL, Li Y, Huang D. Clinical and research applications of anterior segment optical coherence tomography: a review. *Clin Experiment Ophthalmol*. 2009; 37:81–89. [PubMed: 19016809]

13. Maldonado MJ, Ruiz-Oblitas L, Munuera JM, et al. Optical coherence tomography evaluation of the corneal cap and stromal bed features after laser in situ keratomileusis for high myopia and astigmatism. *Ophthalmology*. 2000; 107:81–87. [PubMed: 10647724]
14. Li Y, Netto MV, Shekhar R, Krueger RR, Huang D. A longitudinal study of LASIK flap and stromal thickness with high-speed optical coherence tomography. *Ophthalmology*. 2007; 114:1124–1132. [PubMed: 17320959]
15. Skarmoutsos F, Sandhu SS, Voros GM, Shafiq A. The use of optical coherence tomography in the management of cystoid macular edema in pediatric uveitis. *J AAPOS*. 2006; 10:173–174. [PubMed: 16678755]
16. Shields CL, Mashayekhi A, Luo CK, Materin MA, Shields JA. Optical coherence tomography in children: analysis of 44 eyes with intraocular tumors and simulating conditions. *J Pediatr Ophthalmol Strabismus*. 2004; 41:338–344. [PubMed: 15609518]
17. Meyer CH, Lapolice DJ, Freedman SF. Foveal hypoplasia in oculocutaneous albinism demonstrated by optical coherence tomography. *Am J Ophthalmol*. 2002; 133:409–410. [PubMed: 11860983]
18. Harvey PS, King RA, Summers CG. Spectrum of foveal development in albinism detected with optical coherence tomography. *J AAPOS*. 2006; 10:237–242. [PubMed: 16814177]
19. El-Dairi MA, Holgado S, O'Donnell T, Buckley EG, Asrani S, Freedman SF. Optical coherence tomography as a tool for monitoring pediatric pseudotumor cerebri. *J AAPOS*. 2007; 11:564–570. [PubMed: 17920318]
20. El-Dairi MA, Holgado S, Asrani SG, Enyedi LB, Freedman SF. Correlation between optical coherence tomography and glaucomatous optic nerve head damage in children. *Br J Ophthalmol*. 2009; 93:1325–1330. [PubMed: 19028739]
21. El-Dairi MA, Asrani SG, Enyedi LB, Freedman SF. Optical coherence tomography in the eyes of normal children. *Arch Ophthalmol*. 2009; 127:50–58. [PubMed: 19139338]
22. Ecsedy M, Szamosi A, Karko C, et al. A comparison of macular structure imaged by optical coherence tomography in preterm and full-term children. *Invest Ophthalmol Vis Sci*. 2007; 48:5207–5211. [PubMed: 17962475]
23. Dickmann A, Petroni S, Salerno A, Dell'Omo R, Balestrazzi E. Unilateral amblyopia: an optical coherence tomography study. *J AAPOS*. 2009; 13:148–150. [PubMed: 19157939]
24. Querques G, Bux AV, Iaculli C, Delle Noci N. Isolated foveal hypoplasia. *Retina*. 2008; 28:1552–1553. [PubMed: 18997616]
25. Patel CK. Optical coherence tomography in the management of acute retinopathy of prematurity. *Am J Ophthalmol*. 2006; 141:582–584. [PubMed: 16490519]
26. Joshi MM, Trese MT, Capone A Jr. Optical coherence tomography findings in stage 4A retinopathy of prematurity: a theory for visual variability. *Ophthalmology*. 2006; 113:657–660. [PubMed: 16581425]
27. Harris PD, Farmery AD, Patel CK. The challenges of positioning an infant undergoing optical coherence tomography under general anesthesia. *Paediatr Anaesth*. 2009; 19:64–65. [PubMed: 19076521]
28. Scott AW, Farsiu S, Enyedi LB, Wallace DK, Toth CA. Imaging the infant retina with a hand-held spectral-domain optical coherence tomography device. *Am J Ophthalmol*. 2009; 147:364–373.e2. [PubMed: 18848317]
29. Muni RH, Kohly RP, Sohn EH, Lee TC. Hand-held spectral domain optical coherence tomography finding in shaken-baby syndrome. *Retina*. 2010; 30(4 suppl):S45–S50. [PubMed: 20386092]
30. Chong GT, Farsiu S, Freedman SF, et al. Abnormal foveal morphology in ocular albinism imaged with spectral-domain optical coherence tomography. *Arch Ophthalmol*. 2009; 127:37–44. [PubMed: 19139336]
31. Muni RH, Kohly RP, Charonis AC, Lee TC. Retinoschisis detected with handheld spectral-domain optical coherence tomography in neonates with advanced retinopathy of prematurity. *Arch Ophthalmol*. 2010; 128:57–62. [PubMed: 20065217]
32. Chavala SH, Farsiu S, Maldonado R, Wallace DK, Freedman SF, Toth CA. Insights into advanced retinopathy of prematurity using hand-held spectral domain optical coherence tomography imaging. *Ophthalmology*. 2009; 116:2448–2456. [PubMed: 19766317]

33. Gerth C, Zawadzki RJ, Heon E, Werner JS. High-resolution retinal imaging in young children using a handheld scanner and Fourier-domain optical coherence tomography. *J AAPOS*. 2009; 13:72–74. [PubMed: 19121595]
34. Maldonado RS, Izatt JA, Sarin N, et al. Optimizing hand-held spectral domain optical coherence tomography imaging for neonates, infants, and children. *Invest Ophthalmol Vis Sci*. 2010; 51:2678–2685. [PubMed: 20071674]
35. Berrocal AM, Houston SK, Pina Y, Murray TG. Bascom Palmer Imaging Group. Intraoperative spectral domain optical coherence tomography (SD-OCT) imaging of complex pediatric retinal disease. *ARVO Meeting Abstracts*. 2010; 51:3861.
36. Vinekar A, Sivakumar M, Shetty R, et al. A novel technique using spectral-domain optical coherence tomography (Spectralis, SD-OCT+HRA) to image supine non-anaesthetized infants: utility demonstrated in aggressive posterior retinopathy of prematurity. *Eye (Lond)*. 2010; 24:379–382. [PubMed: 20057510]
37. Baranano DE, Fortun JA, Ray R, et al. Intraoperative spectral-domain optical coherence tomography for macular pucker surgery. *ARVO Meeting Abstracts*. 2010; 51:269.
38. Ray R, Baranano DE, Fortun JA, et al. Intraoperative microscope mounted spectral domain optical coherence tomography for evaluation of retinal anatomy during macular surgery. *Ophthalmology*. In press.
39. Dayani PN, Maldonado R, Farsiu S, Toth CA. Intraoperative use of handheld spectral domain optical coherence tomography imaging in macular surgery. *Retina*. 2009; 29:1457–1468. [PubMed: 19823107]
40. Wykoff CC, Berrocal AM, Scheffler AC, Uhlhorn SR, Ruggieri M, Hess D. Intraoperative OCT of a full-thickness macular hole before and after internal limiting membrane peeling. *Ophthalmic Surg Lasers Imaging*. 2010; 41:7–11. [PubMed: 20128563]
41. Lee LB, Srivastava S. Intraoperative spectral domain imaging of rhegmatogenous retinal detachment repair using perfluoro-n-octane tamponade. *ARVO Meeting Abstracts*. 2010; 51:6076.
42. Knecht PB, Kaufmann C, Menke MN, Watson SL, Bosch MM. Use of intraoperative fourier-domain anterior segment optical coherence tomography during descemet stripping endothelial keratoplasty. *Am J Ophthalmol*. 2010; 150:360–365. [PubMed: 20591396]
43. Ide T, Wang J, Tao A, et al. Intraoperative use of three-dimensional spectral-domain optical coherence tomography. *Ophthalmic Surg Lasers Imaging*. 2010; 41:250–254. [PubMed: 20307045]
44. Tao YK, Ehlers JP, Toth CA, Izatt JA. Intraoperative spectral domain optical coherence tomography for vitreoretinal surgery. *Opt Lett*. 2010; 35:3315–3317. [PubMed: 20967051]
45. Delori FC, Webb RH, Sliney DH. Maximum permissible exposures for ocular safety (ANSI 2000), with emphasis on ophthalmic devices. *J Opt Soc Am A Opt Image Sci Vis*. 2007; 24:1250–1265. [PubMed: 17429471]
46. Sliney D, Aron-Rosa D, DeLori F, et al. Adjustment of guidelines for exposure of the eye to optical radiation from ocular instruments: statement from a task group of the International Commission on Non-Ionizing Radiation Protection (ICNIRP). *Appl Opt*. 2005; 44:2162–2176. [PubMed: 15835362]
47. American National Standard Institute. *American National Standard for Safe Use of Laser*. New York: Author; 2007.
48. Ehlers JP, Tao YK, Maldonado R, Izatt J, Toth CA. Intraoperative integration of a microscope mounted spectral domain optical coherence tomography system [published online ahead of print January 31, 2011]. *Invest Ophthalmol Vis Sci*.
49. Binder S, Falkner-Radler CI, Hauger C, Matz H, Glittenberg CG. Clinical applications of intrasurgical SD-optical coherence tomography. *ARVO Meeting Abstracts*. 2010; 51:268.
50. Han S, Sarunic MV, Wu J, Humayun M, Yang C. Handheld forward-imaging needle endoscope for ophthalmic optical coherence tomography inspection. *J Biomed Opt*. 2008; 13:020505. [PubMed: 18465947]
51. Balicki M, Han JH, Iordachita I, et al. Single fiber optical coherence tomography microsurgical instruments for computer and robot-assisted retinal surgery. *Med Image Comput Comput Assist Interv*. 2009; 12:108–115. [PubMed: 20425977]

52. Radhakrishnan S, Rollins AM, Roth JE, et al. Real-time optical coherence tomography of the anterior segment at 1310 nm. *Arch Ophthalmol*. 2001; 119:1179–1185. [PubMed: 11483086]
53. Geerling G, Muller M, Winter C, et al. Intraoperative 2-dimensional optical coherence tomography as a new tool for anterior segment surgery. *Arch Ophthalmol*. 2005; 123:253–257. [PubMed: 15710824]
54. Huttmann G, Lankenau E, Schulz-Wackerbarth C, Muller M, Steven P, Birngruber R. Optical coherence tomography: from retina imaging to intraoperative use: a review [article in German]. *Klin Monbl Augenheilkd*. 2009; 226:958–964. [PubMed: 20108189]
55. Kermani O, Will F, Massow O, Oberheide U, Lubatschowski H. Control of femtosecond thin-flap LASIK using OCT in human donor eyes. *J Refract Surg*. 2010; 26:57–60. [PubMed: 20199014]
56. Ehlers JP, Gupta PK, Farsiu S, et al. Evaluation of contrast agents for enhanced visualization in optical coherence tomography. *Invest Ophthalmol Vis Sci*. 2010; 51:6614–6619. [PubMed: 21051711]
57. Galeotti J, Sajjad A, Wang B, et al. The OCT penlight: in-situ image guidance for microsurgery. *Proc SPIE*. 2010; 7625:762502.

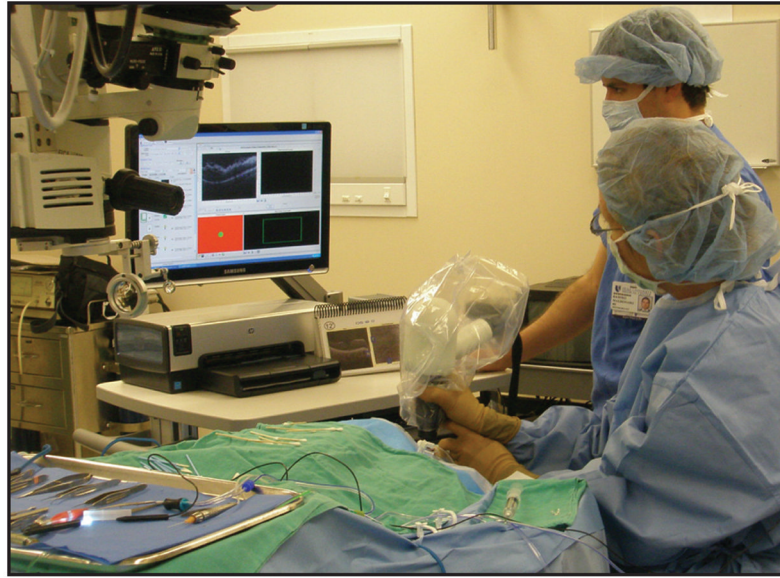


Figure 1.

Intraoperative use of the handheld Bioptigen spectral-domain optical coherence tomography (SD-OCT) scanner (Bioptigen, Inc., Research Triangle Park, NC). The surgeon is holding the handheld SD-OCT scanner to quickly obtain high-resolution SD-OCT images under sterile conditions in the operating room immediately following surgical maneuvers. The surgical microscope has been positioned away from the surgical field to permit imaging. The mobile OCT computing station and the assistant controlling the OCT software are visible to the right of the surgeon.

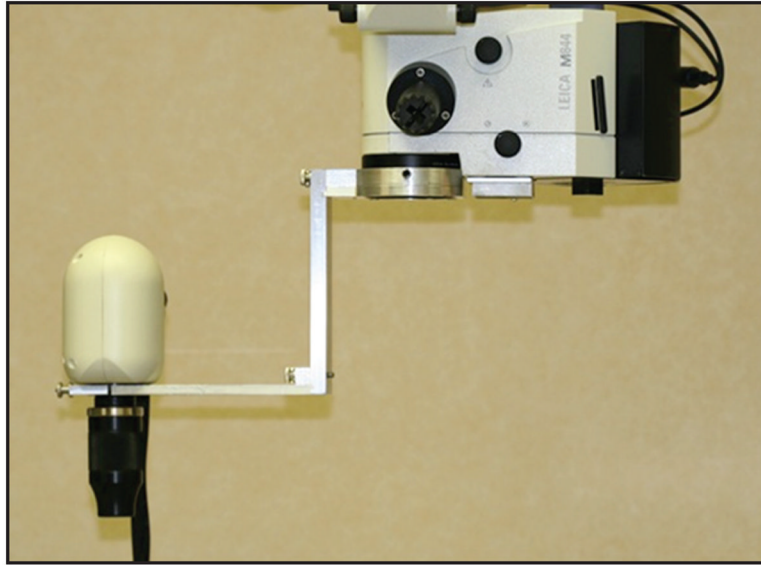


Figure 2. Handheld Bioptigen spectral-domain optical coherence tomography scanner (Bioptigen, Inc., Research Triangle Park, NC) stabilized with custom microscope armature. The scanner can be pivoted in and out of imaging position for increased imaging efficiency and stabilization. (Image provided by Sunil Srivastava, MD)

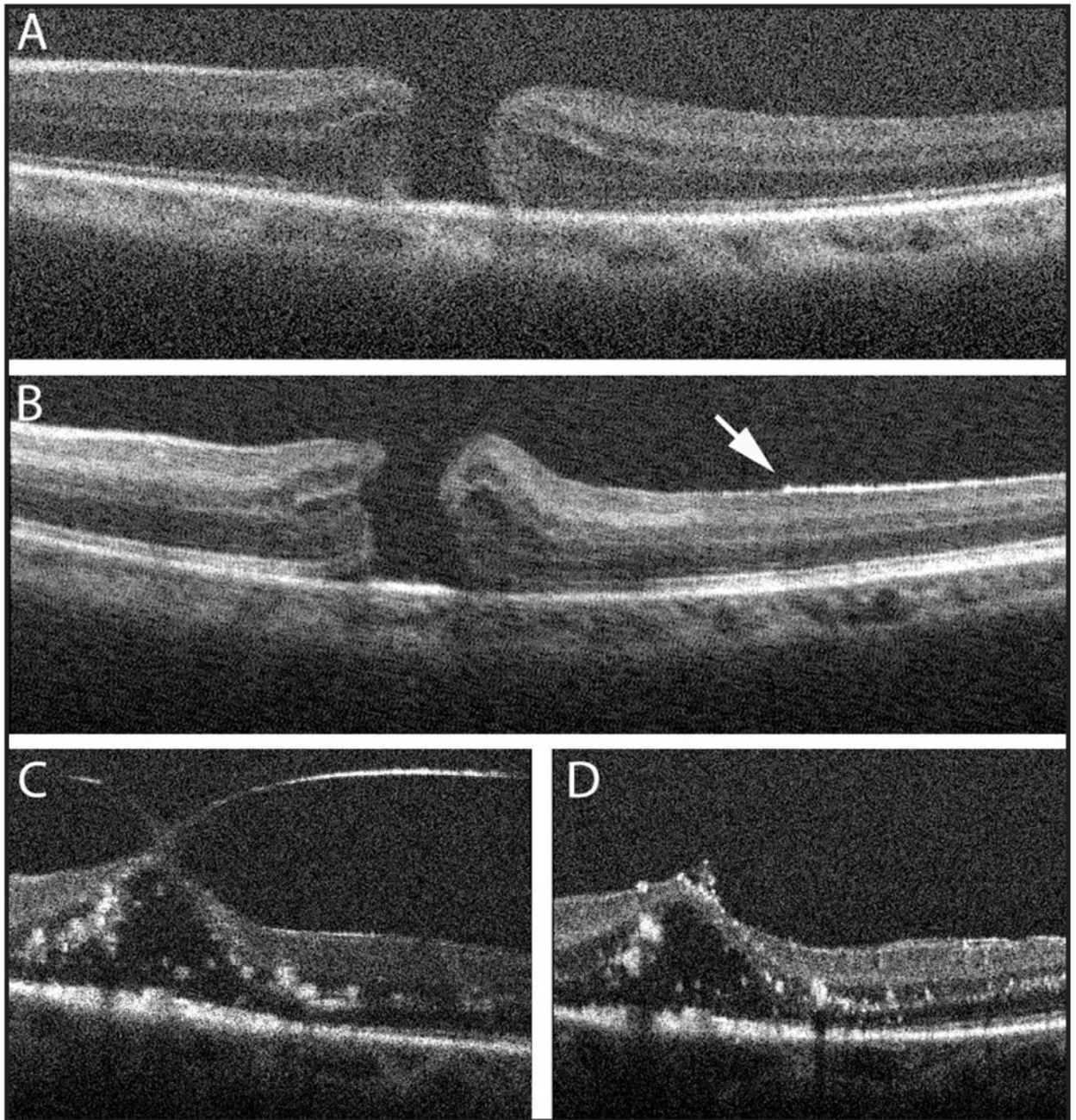


Figure 3.

Comparison of preoperative and intraoperative hand-held spectral-domain optical coherence tomography images in two patients undergoing vitreoretinal surgery for macular hole (A, B) and for vitreomacular traction (C, D). In the patient with a macular hole, preoperative images demonstrate a full-thickness macular hole with mild cystic thickening (A). Immediately following internal limiting membrane (ILM) peel (B), the elevated appearance of the edges of the hole suggests reduced tangential traction. Residual ILM can be visualized as a hyperreflective band on the inner retinal surface, whose absence (arrow) marks the area of peeled ILM. In the patient with vitreomacular traction, preoperative images demonstrate traction and elevation on the fovea by prominent vitreous adhesions (C), which are no longer

observed following successful hyaloid peeling (D). (Reprinted with permission from Dayani PN, Maldonado R, Farsiu S, Toth CA. Intraoperative use of handheld spectral domain optical coherence tomography imaging in macular surgery. *Retina*. 2009;29:1457–1468.)

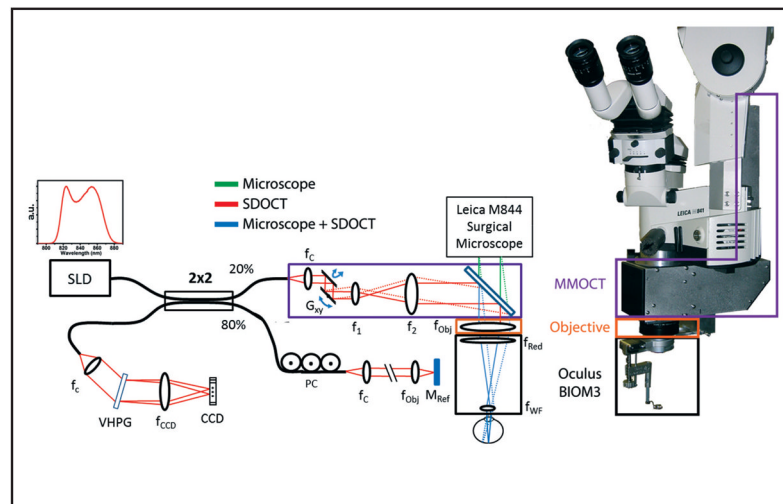


Figure 4. Optical schematic and photograph of the microscope-mounted optical coherence tomography (MM-OCT) system mounted on a Leica surgical microscope. The optical paths of the surgical microscope (green) and spectral-domain optical coherence tomography (SD-OCT) (red) are shown along with the shared path (blue). The MM-OCT optics (purple box) consist of galvanometer scanners, a beam-expanding telescope, a dichroic beamsplitting mirror, and focusing optics from the surgical microscope including a microscope objective (orange box) and reduction and widefield ophthalmic lenses (black box). CCD = linear CCD array; PC = polarization controller; VHPG = volume phase holographic grating; SLD = super-luminescent diode; G = galvanometer.

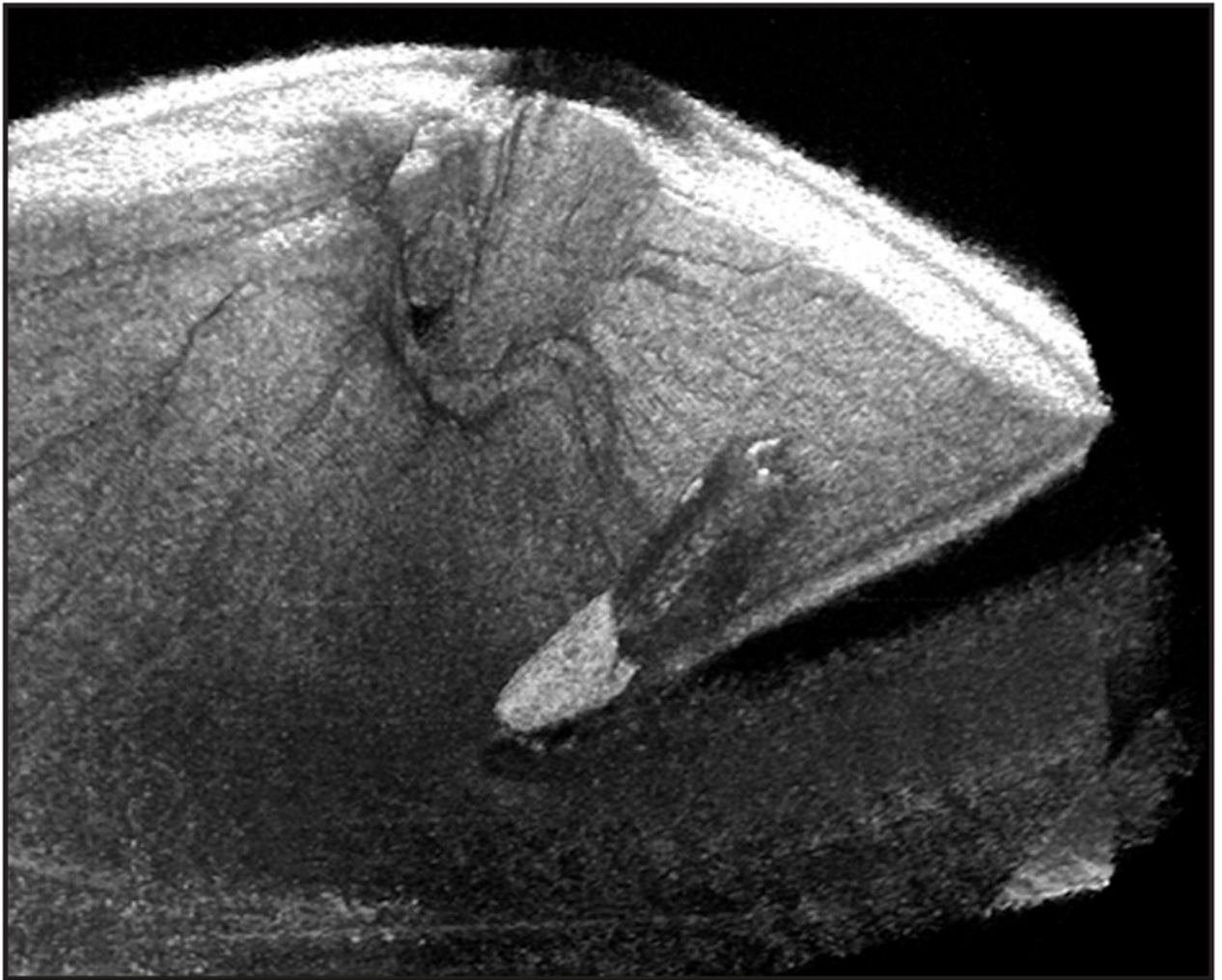


Figure 5.

Microscope-mounted optical coherence tomography (MM-OCT) obtained volumetric rendering of surgical manipulation with the diamond-dusted Tano scraper in a cadaveric porcine eye. The surgical procedure was performed while viewing through the surgical microscope with concurrent acquisition of MM-OCT B-scans. Volumetric renderings allow three-dimensional visualization of the instrument and retina. Shadowing from the instruments obscures visualization of the directly underlying retina. (Reprinted with permission from Ehlers JP, Tao YK, Maldonado R, Izatt J, Toth CA. Intraoperative integration of a microscope mounted spectral domain optical coherence tomography system [published online ahead of print January 31, 2011]. *Invest Ophthalmol Vis Sci*. ©Association for Research in Vision & Ophthalmology).

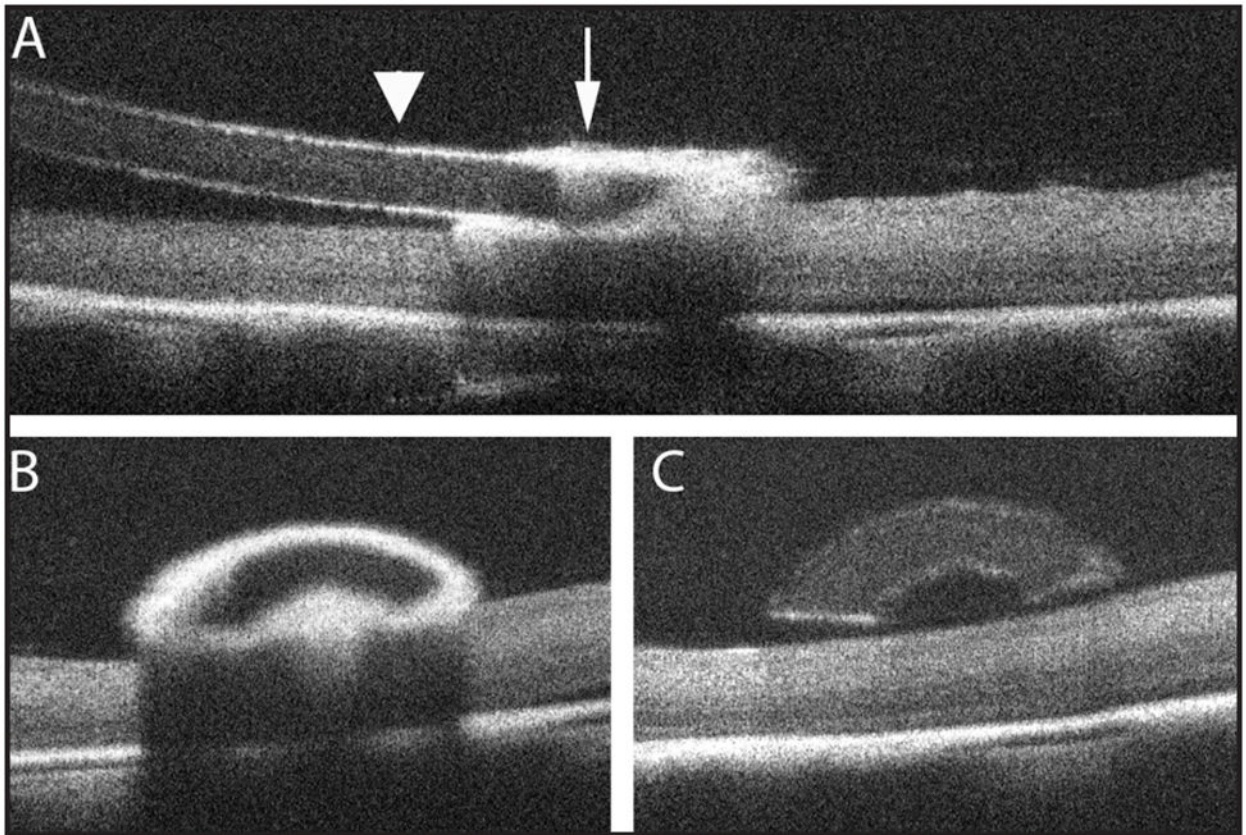


Figure 6.

Microscope-mounted optical coherence tomography obtained B-scans of surgical manipulation with the diamond-dusted silicone Tano scraper in a cadaveric porcine eye. A single B-scan along the longitudinal axis of the Tano scraper (A) demonstrates a highly reflective diamond-dusted tip (arrow) causing significant underlying shadowing of the retina with improved retinal visibility under the non-diamond-dusted silicone shaft (arrowhead). A single B-scan perpendicular to and passing through the diamond-dusted tip (B; corresponds to the level of the arrow in A) demonstrates the arcuate appearance of the Tano scraper and highlights the increased reflectivity and limited transmission through the diamond-dusted tip. A single B-scan perpendicular to and passing through the silicone shaft of the Tano scraper (C; corresponds to the level of the arrowhead in A) further illustrates the arcuate shape of the instrument and demonstrates improved visibility of underlying retinal structures.